Paper: ASAT-16-092-ST

16th International Conference on
AEROSPACE SCIENCES & AVIATION TECHNOLOGY,
ASAT - 16 – May 26 - 28, 2015, E-Mail: asat@mtc.edu.eg
Military Technical College, Kobry Elkobbah, Cairo, Egypt
Tel : +(202) 24025292 – 24036138, Fax: +(202) 22621908

Direct Prediction of Failure in Bonded Composite Lap Joints under Shear Load

A. OKASHA EL-NADY*

ABSTRACT

A simple and accurate formula to calculate the failure load of adhesive bonded single lap joints under shear load based on plastic-to-failure criterion is presented. For this purpose a new failure mechanism is proposed, in which it is assumed that there is a critical lap length at which the adhesive behavior is perfectly plastic along the lap length.
Solution of the governing differential equation is obtained in the elastic and plastic ranges. Straightforward arrangements of the boundary and compatibility conditions yield an explicit formula for the critical lap length, and hence a closed formula for the failure load can be found. The failure loads using the proposed analytical solution are calculated and compared with published results obtained using the numerical Runge-Kutta fourth order with shooting method. The comparison shows that the analytical solution predicts failure loads for a carbon/epoxy adherend joint within a 3.5% error, and within 1.8 for a glass/epoxy adherend joint. Also the failure loads corresponding to the critical lap lengths are calculated using the derived closed formula and compared with the published results. The comparison shows that these failure loads accurately predict the plastic failure limit within 2.6% for a carbon/epoxy adherend joint and within 4.7% for glass/epoxy adherend joint, for lap lengths greater than the critical one. Example calculations presented in this paper show that the critical failure loads can be considered as a conservative prediction of joint failure since they are always less than the upper limit of the failure loads.

KEYWORDS: Adhesively bonded joint; failure prediction; in-plane shear; critical lap length

INTRODUCTION

Adhesive bonding has been applied successfully in many technologies. Adhesive bonding of structures has significant advantages over conventional fastening systems. Bonded joints are considerably more fatigue resistant than mechanically fastened structures [1] because of the absence of stress concentrations that occur at fasteners. Joints may be lighter due to the absence of fastener hardware. Adhesive bonding may also be used for repairs to metallic structures and offers even further advantages over mechanically fastened repairs. Bonded composite repairs are efficient and cost-effective means of repairing cracks and corrosion grind-out cavities in metallic and composite structures.
The disadvantages of an adhesive-bonded joint include the fact that it is a single fastener, and hence, there is no redundancy of load paths unless alternative load paths are added. [2].

* Lecturer, Mechatronics Department, Faculty of Engineering, O6U, 6th October City, Giza, Egypt.

The foremost applications where primary loaded structures rely on adhesive bonding are aircraft and space structures. Some examples are the fuselage splice joint and the bonded wing leading edge. These structures carry significant torque loads in the form of in-plane shear flow that must be transferred across the joints. Generally, adhesively bonded lap joint loaded by in-plane shear is a generic structural configuration in bonded composite assemblies.

The growing applications of adhesive bonding in aircraft structures require more emphasis on analytical models to predict failure and load carrying capability. In general, bonded composite structures are designed to be loaded only up to their elastic limit. However, when designing for ultimate load, if the structure can operate to the joint's failure limit, the structure can be used more efficiently.

The analytical treatment of a bonded lap joint where the adherends are loaded in tension has been considered extensively by many authors. Hart-Smith [3, 4] extended the shear-lag model that was presented by Volkersen [5] to include elastic-to-perfectly plastic adhesive behavior. Goland and Reissner [6] and Oplinger [7] accounted for adherend bending deflections to predict the peel stress in the adhesive. Tsai, Oplinger, and Morton [8] provided a correction for adherend shear deformation, resulting in a simple modification of the Volkersen's theory basic equations. Nguyen and Kedward [9] introduced a nonlinear adhesive constitutive model composed of three fitting parameters and used it to predict the adhesive shear strain distribution of a tubular adhesive scarf joint loaded to failure in tension.

Adhesively bonded lap geometries loaded by in-plane shear have been discussed by Hart-Smith [3], van Rijn [10], and the Engineering Sciences Data Unit [11]. The authors of these works indicate that shear loading can be analytically accounted for by simply replacing the adherend Young's moduli in the tensile loaded lap joint solution with the respective adherend shear moduli. This assumption is valid only for simple cases with one dimensional loading; whereas in-plane shear loaded joints are generally two or three dimensional.

Although finite element analysis (FEA) can be applied to predict failure limit accurately, FEA is a time consuming process and may not easily be performed for all joint configurations. Due to the inherent three-dimensional nature of the joint geometry and shear loading conditions, three-dimensional elements need to be used in FEA modeling of shear flow transfer across a lap joint. Creating a mesh having sufficient element refinement to capture the high stress gradients in the thin adhesive layer can easily result in a FEA model of unsolvable size. Failure limit load predictions by simple theoretical methods are therefore quite useful if they can provide accurate predictions for much less effort than FEA.

Kim and Lee [12] established a theoretical model that predicts failure in adhesively bonded lap joints loaded by in-plane shear. The model is based on shear lag assumptions and accounts for a nonlinear adhesive shear stress-strain relationship. The nonlinear adhesive constitutive model composed of two fitting parameters of Nguyen and Kedward [9] is used in the derivation of the governing differential equation. The governing equation cannot be solved directly, so, the numerical Runge-
Kutta fourth order with shooting method [13] is applied to obtain a solution. Failure of the joint is determined when the plastic strain reaches its ultimate value.

In this paper a simple and accurate formula to calculate the failure load of adhesive bonded joints under shear load based on plastic-to-failure criterion is presented. For this purpose a new failure mechanism is proposed. According to this mechanism, there is a critical lap length at which the adhesive behavior is perfectly plastic along the lap length. So, the theoretical model presented in [12] is extended to directly predict the failure limit of in-plane shear loaded adhesively bonded joints. The nonlinear adhesive behavior is accounted for using the two parameter version of Nguyen and Kedward [9]. The fitted curve is idealized

to the elastic-perfectly plastic model recommended by Hart-Smith [3] to obtain the elastic failure limit. The exact solution of the governing differential equation is obtained in the elastic and plastic ranges. Arrangements of the boundary and compatibility conditions yield an explicit formula for the critical lap length, at which the adhesive behavior is perfectly plastic along the lap length, and hence a closed formula for the failure load is obtained.

The failure loads using the presented analytical solution are calculated and compared with published results obtained by using the numerical Runge-Kutta fourth order with shooting method. The comparison shows that the analytical solution predicts failure loads accurately for a carbon/epoxy adherend joint within 3.5%, and within 1.8 for a glass/epoxy adherend joint. Also the failure loads corresponding to the critical lap lengths are calculated using the derived closed formula and compared with the published results corresponding to lap length greater than the critical one. The comparison shows that these failure loads accurately predict the plastic failure limit within 2.6% for a carbon/epoxy adherend joint and within 4.7% for glass/epoxy adherend joint. Examples calculations presented in this paper show that the critical failure loads can be considered as a conservative prediction of joint failure since they are always less the upper limit of the failure loads.

GOVERNING EQUATION

The governing equation for the one dimensional single lap joint shown in Fig. 1, under shear load N_{xy} as presented in [12] is given by:

$$\frac{d^2\gamma_{yz}}{dx^2} = \frac{1}{t_a}\left(\frac{1}{G_o t_o} + \frac{1}{G_i t_i}\right)\tau_{yz}$$

where; G_o, G_i … Young's modulus in shear of the outer and inner adhereneds respectively.
t_o, t_i … thickness of the outer and inner adhereneds respectively.

In the following the subscript yz, for brevity is canceled. So, the governing equation becomes:

$$\frac{d^2\gamma}{dx^2} = \frac{1}{t_a}\left(\frac{1}{G_o t_o} + \frac{1}{G_i t_i}\right)\tau \qquad (1)$$

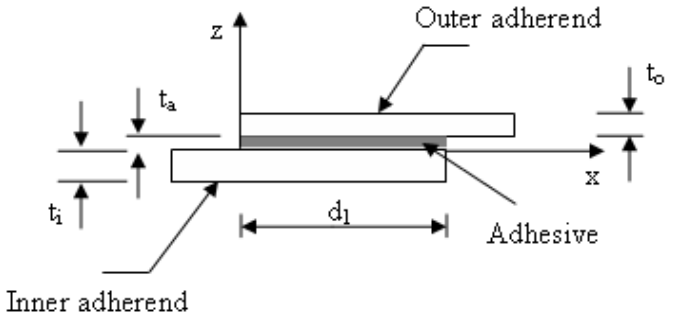

Fig. 1 One dimensional single lap joint

The constitutive behavior for a ductile adhesive described by a two-parameter model is given by [12]:

$$\tau = (G - kB_1)\gamma + B_1(1 - e^{-k\gamma}) \qquad (2)$$

where k and B_1 are the fitting parameters.

Equation (2) is leveled as follows;

$$\gamma_{pf} = \gamma_{ult}$$

$$\tau_{ef} = \tau_p \qquad (3)$$

$$G\,\gamma_{ef} = (G - kB_1)\gamma_{ult} + B_1(1 - e^{-k\gamma_{ult}})$$

and shown in Fig. 2:

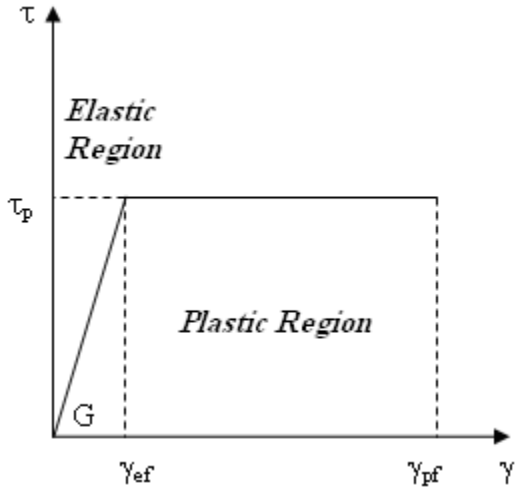

Fig. 2 leveling of constitutive behavior

From equation (3) the shear strain at the elastic limit γ_{ef} is calculated. The solution of equation (1) depends on the behavior of the adhesive shear strain.

Elastic Analysis

In the elastic region;

$$\tau = G\,\gamma_e; \qquad \gamma = \gamma_e$$

$$\frac{d^2\gamma_e}{dx^2} = \lambda^2\gamma_e \qquad \lambda^2 = \frac{G}{t_a}\left(\frac{1}{G_o t_o} + \frac{1}{G_i t_i}\right) \qquad (4)$$

The solution is:

$$\gamma_e = C_1 \sinh \lambda x + C_2 \cosh \lambda x \qquad (5)$$

Plastic Analysis

In the plastic region;

$$\tau = G\,\gamma_{ef}; \qquad \gamma = \gamma_p$$

$$\frac{d^2\gamma_p}{dx^2} = \lambda^2\,\gamma_{ef} \tag{6}$$

The solution is:

$$\gamma_p = \tfrac{1}{2}\,\lambda^2\,\gamma_{ef}\,x^2 + C_3\,x + C_4 \tag{7}$$

The constants C_1, C_2, C_3, and C_4 are determined from the boundary and compatibility conditions.

The shear strain of the adhesive under shear loads behaves in plastic-elastic-plastic manner as shown in Fig. 3.
The shear strain distribution in the plastic region p_1 is given by equation (7) while it is given by equation (5) in the elastic region. The distribution in the plastic region p_2 is given by equation (8):

$$\gamma_{p2} = \tfrac{1}{2}\,\lambda^2\,\gamma_{ef}\,x^2 + C_5\,x + C_6 \tag{8}$$

Boundary Conditions:

1) $$\left.\frac{d\gamma_{p1}}{dx}\right|_{x=0} = -\frac{N_{xy}}{t_a G_i t_i}$$

2) $$\left.\frac{d\gamma_{p2}}{dx}\right|_{x=d1} = \frac{N_{xy}}{t_a G_o t_o}$$

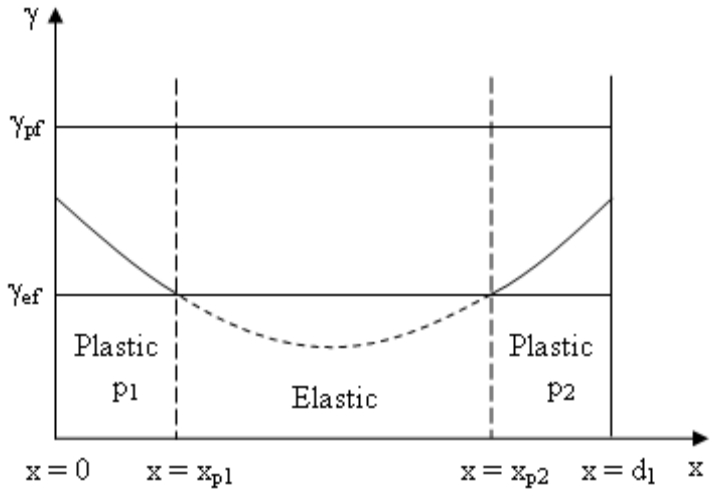

Fig. 2 Shear strain distribution in the adhesive

Compatibility Conditions:

3) $$\gamma_{p1}\Big|_{x=x_{p1}} = \gamma_e\Big|_{x=x_{p1}}$$

4) $$\left.\frac{d\gamma_{p1}}{dx}\right|_{x=x_{p1}} = \left.\frac{d\gamma_e}{dx}\right|_{x=x_{p1}}$$

5) $$\gamma_e\Big|_{x=x_{p1}} = \gamma_{ef}$$

6) $$\gamma_{p2})_{x=x_{p2}} = \gamma_e)_{x=x_{p2}}$$

7) $$\left.\frac{d\gamma_{p2}}{dx}\right|_{x=x_{p2}} = \left.\frac{d\gamma_e}{dx}\right|_{x=x_{p2}}$$

8) $$\gamma_e\Big|_{x=x_{p2}} = \gamma_{ef}$$

There are 8 unknowns C_1, C_2, C_3, C_4, C_5, C_6, x_{p1}, and x_{p2} in 8 equations (2 boundary conditions and 6 compatibility conditions).

Applying boundary conditions 1 and 2 yields:

$$C_3 = -\frac{N_{xy}}{t_a G_i t_i} \tag{9}$$

and;

$$C_5 = \frac{N_{xy}}{t_a G_o t_o} - \lambda^2 \gamma_{ef} d_1 \tag{10}$$

Applying compatibility conditions 4, 5, 7, and 8 yields the following transcendental equation in Δ:

$$2\gamma_{ef}(1-\cosh\lambda\Delta) + \left[\lambda\gamma_{ef}\Delta + \frac{1}{\lambda}(C_5 - C_3)\right]\sinh\lambda\Delta = 0 \tag{11}$$

where Δ is the distance of the elastic region ($\Delta = x_{p2} - x_{p1}$)

The transcendental equation (11) is solved to obtain Δ. Then;

$$x_{p2} = \frac{1}{2}\left(\Delta - \frac{C_5 + C_3}{\lambda^2\gamma_{ef}}\right) \tag{12}$$

$$x_{p1} = x_{p2} - \Delta \tag{13}$$

$$C_1 = \overline{C}_3 \cosh\lambda x_{p1} - \gamma_{ef}\sinh\lambda x_{p1} \tag{14}$$

$$C_2 = \overline{C}_5 \sinh \lambda x_{p1} + \gamma_{ef} \cosh \lambda x_{p1} \quad (15)$$

where $\overline{C}_3 = \lambda \gamma_{ef}\ x_{p1} + \dfrac{C_3}{\lambda}$

$$\overline{C}_5 = -\overline{C}_3 = \lambda \gamma_{ef}\ x_{p1} + \frac{C_5}{\lambda}$$

Applying compatibility conditions 3 and 6 yields C_4 and C_6.

$$C_4 = C_1 \sinh \lambda x_{p1} + C_2 \cosh \lambda x_{p1} - C_3\, x_{p1} - \frac{1}{2}\lambda^2 \gamma_{ef}\, x_{p1}^2 \quad (16)$$

$$C_6 = C_1 \sinh \lambda x_{p2} + C_2 \cosh \lambda x_{p2} - C_5\, x_{p2} - \frac{1}{2}\lambda^2 \gamma_{ef}\, x_{p2}^2 \quad (17)$$

For large Δ, the transcendental equation (11) can be arranged to obtain Δ as follows:

$$\Delta = (C_3 - C_5 + 2\gamma_{ef}\lambda) / \lambda^2 \gamma_{ef} \quad (18)$$

Determination of the critical lap length:

Failure Mechanism

In this mechanism it is assumed that there is a critical lap length at which the adhesive behavior is perfectly plastic along the lap length. For lap length greater than or less than the critical lap length, the strain distribution is as shown in Fig.3.

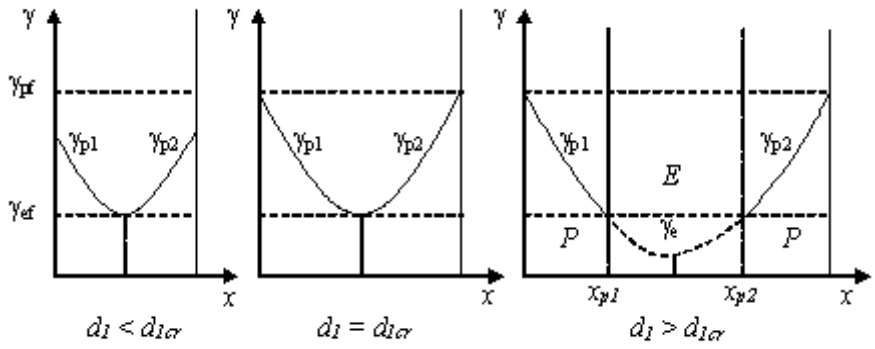

Fig. 3 Failure Mechanism in the Adhesive

From the transcendental equation (11), at the critical condition, i.e. Δ = 0, yields;
(when Δ = 0, $x_{p1} = x_{p2} = d_1/2$)

$C_5 = C_3$

From which

$$N_{xy} = G\gamma_{ef}\ d_1 = \tau_p\, d_{1cr} \quad (19)$$

Also, at this condition, the shear strain at x = 0 (or x = d_1) is,

$$\gamma_{p1}=\gamma_{ult}=C_4=\gamma_{ef}-C_3\frac{d_{1cr}}{2}-\frac{1}{2}\lambda^2\gamma_{ef}\frac{d_{1cr}}{4}$$

Substituting C_3 and rearranging yields for a balanced composite ($G_o t_o = G_i t_i$):

$$d_{1c}=\sqrt{\frac{8(\gamma_{ult}-\gamma_{ef})}{\lambda^2\gamma_{ef}}} \tag{20}$$

Determination of the failure load:

The critical lap length is determined using equation (11). The failure load is calculated using equations (10) as follows:

For $d_1 < d_{1cr}$;

$$(N_{xy})_f = G\gamma_{ef}\, d_1 \tag{21}$$

For $d_1 \geq d_{1cr}$;

$$(N_{xy})_{cr}^{f} = G\gamma_{ef}\, d_{1cr} = \tau_p\sqrt{\frac{8(\gamma_{ult}-\gamma_{ef})}{\lambda^2\gamma_{ef}}} \tag{22}$$

To predict the failure load, the critical lap length is calculated using equation (20). If the overlap length is less than the critical lap length, then the failure load is calculated using equation (21). The shear stain distribution is obtained for the calculated failure load using equations (5), (7), and (8). If the overlap length is greater than the critical lap length, then the failure load is obtained by gradually increasing the applied load N_{xy} and calculating the shear stain distribution using equations (5), (7), and (8) for each given load. The failure load $(N_{xy})^f$ is caught when the shear strain at the ends reaches the ultimate one. The solution algorithm is shown in Fig. 4.The critical failure load can be obtained directly using equation (22). The shear stress distribution can be obtained using equation (2).

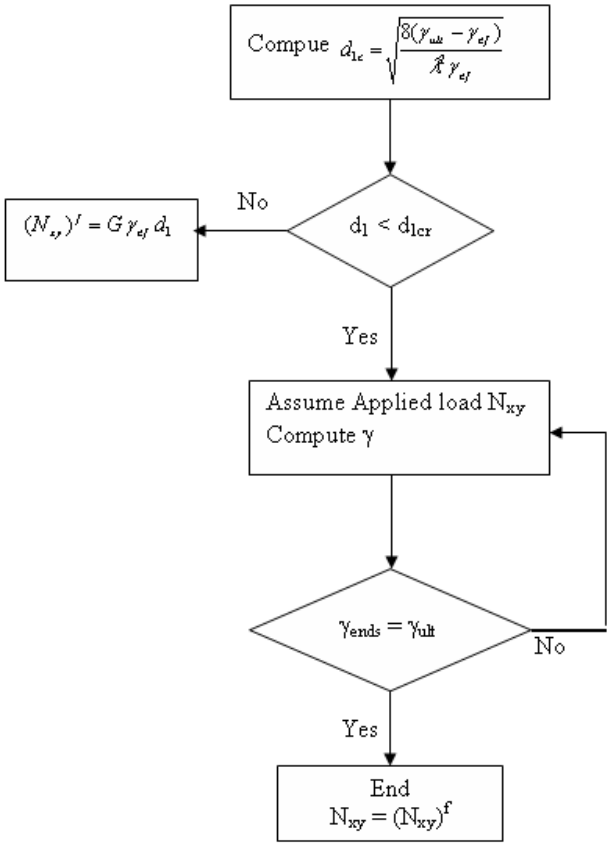

Fig. 4 Solution algorithm

MODEL VALIDATION

To validate the suggested failure mechanism, failure loads are calculated for two joints with carbon/epoxy and glass/epoxy cloth adherends bonded by PTM&W ES6292 adhesive suggested in ref. [12]. Joint parameters are listed in Table 1. The failure load and the critical failure load for two different lap lengths and three different adhesive thicknesses are presented in Table 2 and Table 3.

Table 1 Joint parameters for carbon/epoxy and glass/epoxy adherends

Joint Parameters	carbon/epoxy adherends	glass/epoxy adherends
Lay up	$[0/45/90/-45]_{2s}$	$[0_4/45/-45/0_4]$
t_o, t_i (mm)	2.03	2.49
G_o, G_i (GPa)	22.03	10.07
d_1 (mm)	25.4 and 50.8	
t_a (mm)	0.33, 1.07 and 2.08	
G_a (GPa)	0.927	
τ_{ult} (MPa)	26.3	
γ_{ult}	0.35	

Table 2 Ref.[12] and present results comparisons of Carbon/Epoxy joints.
Adhesive PTM&W ES6292

Critical lap length (d_{1cr})(mm)	t_a (mm)	Failure Limit, $(N_{xy})^f$ (N/mm)					
		l = 25.4 mm			l = 50.8 mm		
		Ref [12]	Present	Critical	Ref [12]	Present	Critical
26.9	0.33	655.5	666.85	706.07	725.1	721.45	706.07
40.6	1.07	630.5	630.34	1007.3	1005	1035.4	1007.3
42.0	2.08	565.4	557.39	931.42	936.9	969.98	931.42

Table 3 Ref. [12] and present results comparisons of Glass/Epoxy joints.
Adhesive PTM&W ES6292

Critical lap length (d_{1cr})(mm)	t_a (mm)	Failure Limit, $(N_{xy})^f$ (N/mm)					
		l = 25.4 mm			l = 50.8 mm		
		Ref [12]	Present	Critical	Ref [12]	Present	Critical
20.1	0.33	541.1	536.90	528.70	543.9	537.74	528.70
30.4	1.07	631.3	630.34	754.29	778.6	777.37	754.29
31.5	2.08	577.9	567.29	702.47	737.3	740.59	702.47

It is clear from the tables that there is good agreement between the results obtained by Runge-Kutta fourth order method [12] and the present analytical method for different lap lengths and adhesive thicknesses. Also, the comparison shows that the analytical solution predicts failure loads accurately for a carbon/epoxy adherend joint within 3.5%, and within 1.8 for a glass/epoxy adherend joint. The failure loads corresponding to the critical lap lengths accurately predict the plastic failure limit within 2.6% for a carbon/epoxy adherend joint and within 4.7% for glass/epoxy adherend joint. The critical failure loads can be considered as a conservative prediction of joint failure since they are always lower than those obtained by analytical method.

The adhesive shear strain (γ) distribution for joints with Carbon/Epoxy adherends at the failure load for different adhesive materials with different lap length are given in Fig. 5. It is clear from the distribution that for lower lap lengths (less than the critical one), the adhesive constitutive behavior is perfectly plastic and the maximum adhesive shear strain does not reach the ultimate plastic one (γ_{pf}). For lap lengths equal to the critical one, the adhesive constitutive behavior is perfectly plastic and the maximum adhesive shear strain is equal to the ultimate plastic one (γ_{pf}). For long lap lengths (greater than the critical one), the adhesive constitutive behavior is plastic-elastic-plastic and the range of plasticity is nearly equal to the critical lap length.

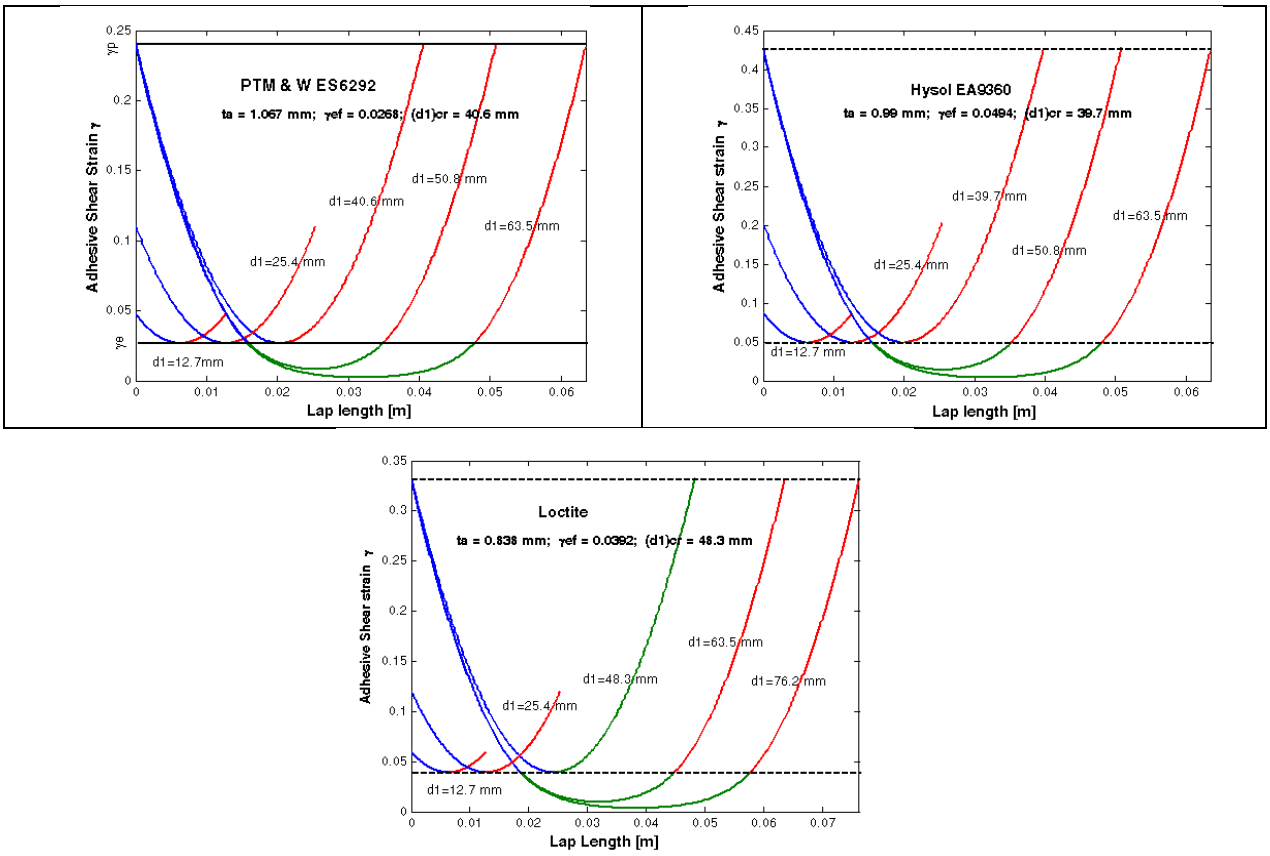

Fig. 5 Adhesive shear strain (γ) distribution for joints with Carbon/Epoxy adherends at the failure load for different adhesive materials with different lap length

CASE STUDIES

The critical lap lengths and the corresponding critical failure loads for three adhesive systems with parameters listed in Table 4 are calculated and reported in Table 5.

Table 4: Adhesive systems parameters

Adhesive	Code	t_a[mm]	k	B_1 [MPa]	γ_{ult}
PTM & W ES6292 G_a=0.927 GPa	PTM1	0.330	36.4	25.367	0.35
	PTM2	1.067	35.6	26.222	0.241
	PTM3	1.829	33.4	29.655	0.073
	PTM4	2.083	36.9	25.829	0.130
	PTM5	3.048	36.8	28.028	0.070
	PTM6	4.267	60.6	14.438	0.031
Hysol EA9360 G_a = 0.855 GPa	Hysol1	0.991	26.2	32.689	0.425
	Hysol2	2.489	23.5	39.708	0.155
Loctite G_a = 0.483 GPa	Loct1	0.838	27.3	17.541	0.334
	Loct2	1.651	21.5	22.671	0.305

Table 5: Critical lap lengths and the corresponding failure loads

Adhesive	t_a[mm]	γ_{ult}	γ_{ef}	C/E $(d_1)_{cr}$ [mm]	G/E $(d_1)_{cr}$ [mm]	C/E $\left(N_{xy}^{pf}\right)_{cr}$ [N/mm]	G/E $\left(N_{xy}^{pf}\right)_{cr}$ [N/mm]
PTM & W ES6292 G_a =0.927GPa	0.330	0.35	0.0283	26.9	20.1	706.07	528.70
	1.067	0.241	0.0268	40.6	30.4	1007.3	754.29
	1.829	0.073	0.0242	26.7	20.0	598.47	448.13
	2.080	0.130	0.0241	42.0	31.5	938.14	702.47
	3.048	0.070	0.0200	38.3	28.7	711.46	532.73
	4.267	0.031	0.0149	29.8	22.3	412.03	308.52
Hysol EA9360 G_a=0.855GPa	0.991	0.425	0.0494	39.7	29.7	1676.5	1255.3
	2.489	0.155	0.0311	45.6	34.1	1210.6	906.46
Loctite G_a =0.483GPa	0.838	0.334	0.0392	48.3	36.2	914.41	684.70
	1.651	0.305	0.0441	60.2	45.05	1280.8	959.07

The failure loads of joints bonded by the previous three adhesive systems with different lap lengths (12.7, 25.4, 38.1, 50.8, 63.5, 76.2, 88.9, and 101.6 mm) are obtained using the present analytical formula and plotted in Figs. 6, 7 and 8 for carbon/epoxy adherends. In these figures the elastic failure loads (N_{xyef} and N_{xyefcr}) are plotted. The elastic failure loads are calculated for different lap lengths using the following formula:

$$N_{xy}^{e} = \frac{2d_1 \tanh(0.5\lambda d_1)}{\lambda d_1} \tag{14}$$

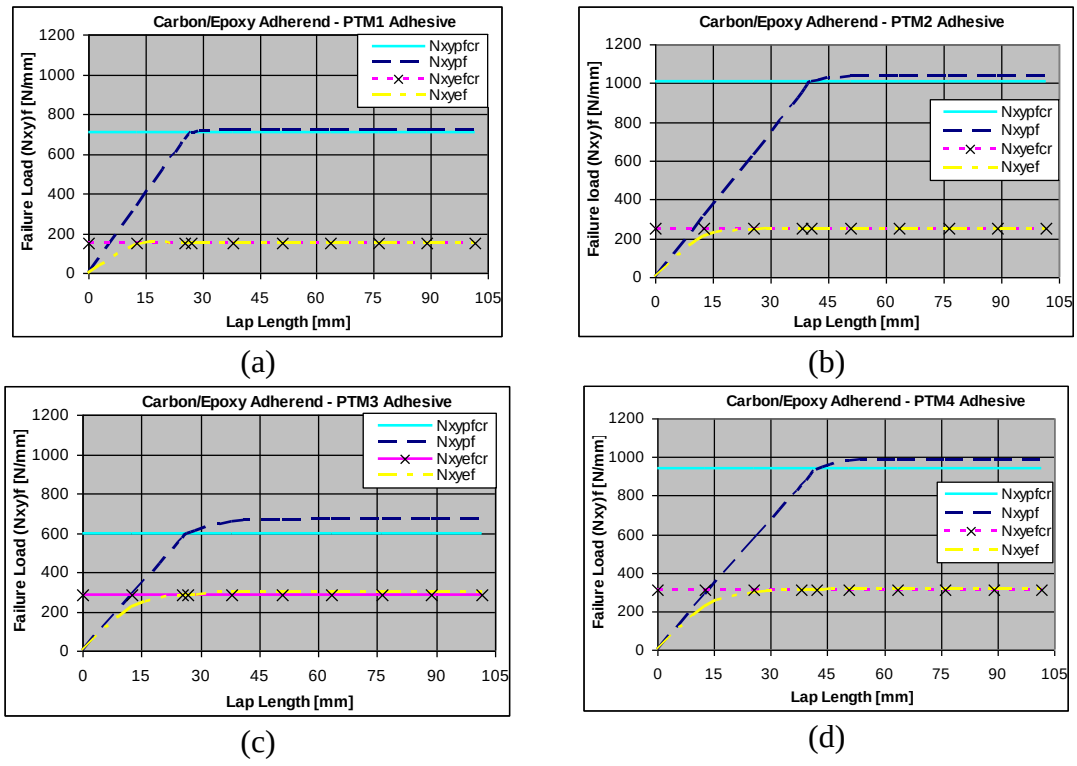

Fig. 6 Failure load distribution for joints with Carbon/Epoxy adherends- PTM & W ES6292 adhesive

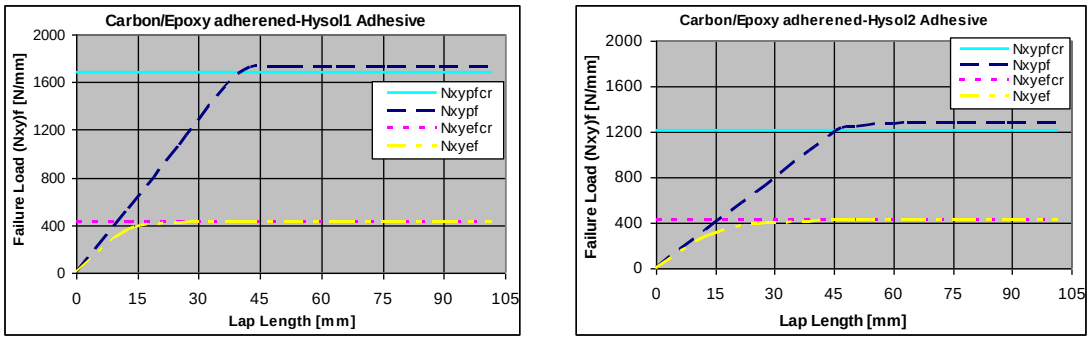

Fig. 7 Failure load distribution for joints with Carbon/Epoxy adherends- Hysol EA9360 adhesive

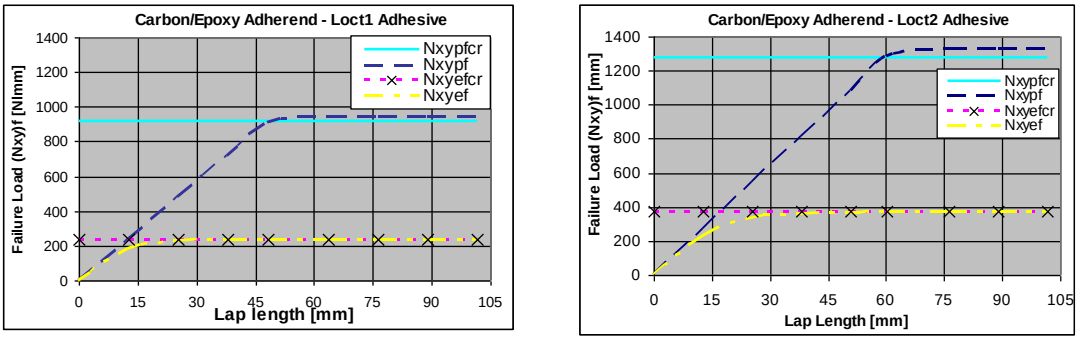

Fig. 8 Failure load distribution for joints with Carbon/Epoxy adherends- Loctite adhesive

Discussion and conclusions

It is clear from equation (20) that the critical lap length depends on the adhesive constitutive behavior (γ_{ef} and γ_{pf}) and the adherends stiffness (Gt). So, each combination of adhesive and adherends has its failure load. This clarifies the reason that predictions of joint failure are non-monotonically dependent on bond line thickness, since adhesive constitutive behavior depends mainly on the bond line thickness.

Equation (21) is a simple formula to calculate the shear failure load which represents the ultimate elastic shear stress in the adhesive per unit lap length.

Tables (2) and (3) show that the critical failure loads have good agreement with results of Ref. [12] for lap lengths greater than the critical one. Figures (6), (7), and (8) show that the critical failure loads are easy and accurate predictions of balanced adhesively bonded joints under shear loads.

The sugested analytical solution predicts failure loads accurately for a carbon/epoxy adherend joint within 3.5%, and within 1.8 for a glass/epoxy adherend joint.
The failure loads corresponding to the critical lap lengths accurately predict the plastic failure limit within 2.6% for a carbon/epoxy adherend joint and within 4.7% for glass/epoxy adherend joint for lap length greater than the critical one. The critical failure loads can be considered as a conservative prediction of joint failure since they are always less the upper limit of the failure loads.

References

1. Hart-Smith, L.J., McDonnell Douglas Corporation Paper MDC 91K0067, August 1991.
2. Baker, A.A., “Crack Patching: Experimental Studies, Practical Applications,” Bonded Repair of Aircraft Structures, A.A. Baker and R. Jones, eds., Martinus Nijhoff, 1988.
3. Hart-Smith, L. J., "Adhesive-Bonded Double-Lap Joints," NASA-Langley Contract Report, NASA-CR-112235, 1973.
4. Hart-Smith, L. J., "Adhesive-Bonded Single-Lap Joints," NASA-Langley Contract Report, NASA-CR-112236, 1973.
5. Volkersen, O., "Die Nietkraftverteilung in Zugbeanspruchten mit Konstanten Laschenquerschritten," Luftfahrtforschung, Vol. 15, 1938, pp. 41-47.
6. Goland, M. and Reissner, E., "The Stresses in Cemented Joints," J. Applied Mechanics, Vol. 11, 1994, pp. A17-A27.
7. Oplinger, D. W. "Effects of Adherend Deflections in Single Lap Joints," Int. J. Solids Structures, Vol. 31, No. 18, 1994, pp. 2565-2587.
8. Tsai, M. Y., Oplinger, D. W., and Morton, J., "Improved Theoretical Solutions for Adhesive Lap Joints," Int. J. Solids Structures, Vol. 35, No. 12, 1998, pp. 1163-1185.
9. Nguyen, V. and Kedward, K. T., "Non-Linear Modeling of Tubular Scarf Joints Loaded in Torsion," Journal of Adhesion, Vol. 76, 2001, pp. 265-292.
10. van Rijn, L. P. V. M., "Towards the Fastenerless Composite Design," Composites PartA, Vol. 27A, 1996, pp. 915-920.
11. Engineering Sciences Data Unit, "Stress Analysis of Single Lap Bonded Joints," Data Item 92041, 1992.
12. Kim, H., and Lee, J., "Adhesive Nonlinearity and the Prediction of Failure in Bonded Composite Lap Joints," Joining and Repair of Composite Structures, ASTM STP 1455, K. T. Kedward and H. Kim, Eds., ASTM International, West Conshohocken, PA, 2004.
13. Conte, S. D. and Boor, C., "Elementary Numerical Analysis - An Algorithm Approach 3 rd edition," McGraw-Hill, pp. 362-372, 412-416, 1981.
14. Kim, H. and Kedward, K. T., "Stress Analysis of Adhesive Bonded Joints Under In-Plane Shear Loading", Journal of Adhesion, Vol. 76, 2001, pp. 1-36.